Dynamic flow, broken surface anchoring, and switching bistability in three-terminal twisted nematic liquid-crystal displays

Tiezheng Qian[a)]
Department of Physics, The Hong Kong University of Science and Technology, Clear Water Bay, Kowloon, Hong Kong

Zhiliang Xie and Hoi S. Kwok
Centre for Display Research, The Hong Kong University of Science and Technology, Clear Water Bay, Kowloon, Hong Kong

Ping Sheng
Department of Physics, The Hong Kong University of Science and Technology, Clear Water Bay, Kowloon, Hong Kong

(Received 12 March 2001; accepted for publication 4 June 2001)

We investigate the switching bistability between the Φ and $\Phi+\pi$ twist states in liquid-crystal cells with a three-terminal electrode structure. Based on general nematohydrodynamic equations and a modeling potential of surface anchoring, numerical calculation shows that dynamic shear flow and electric-field-induced breaking of surface azimuthal anchoring are essential to the realization of the switching bistability observed experimentally. © *2001 American Institute of Physics.*
[DOI: 10.1063/1.1388595]

Bistable twisted nematic (BTN) liquid-crystal (LC) displays have received considerable attention recently. Their display modes are twisted director configurations stabilized through a proper choice of the surface alignment layers and the d/p ratio, where d is the cell thickness and p the helical pitch. Dynamic switching between the Φ and $\Phi+2\pi$ twist states has been demonstrated with strong-anchoring alignment layers,[1–4] while switching between the Φ and $\Phi+\pi$ twist states was realized with the help of breakable *polar* anchorings.[5] Shear flow effects are very important in these BTNs.[3,5,6] More recently, Bryan-Brown reported a twisted nematic display mode based on the use of a grooved surface treated by surfactant.[7]

Unbreakable surface anchoring allows only the $(\Phi,\Phi+2\pi)$ switching in bulk. Therefore, breaking of surface anchoring is essential to the realization of the $(\Phi,\Phi+\pi)$ switching bistability. In this letter, we present a surface-controlled BTN display which employs a structured electrode to produce a near-surface field capable of breaking surface *azimuthal* anchoring.

The present BTN display employs a three-terminal electrode structure consisting of one comb-on-plane (COP) electrode and two planar uniform electrodes.[8] The COP electrode is put on the lower substrate and the two uniform electrodes are on the lower and upper substrates, respectively, as illustrated in Fig. 1. Two voltages can be applied to the COP and the upper planar electrodes, respectively, with the lower planar electrode set to ground. The voltage V_t between the two uniform electrodes produces a vertical electric field. Independently, the voltage V_c between the COP and the lower planar electrodes induces a spatially varying field. This field is near surface, as its strength decays quickly away from the COP surface.[9] The direction of this field is spatially varying but perpendicular to the COP stripes everywhere.[9] Close to the edges of the COP stripes, the electric field has the largest magnitude and is nearly parallel to the COP plane.[9] Strong homogeneous anchoring at the upper substrate is made by rubbing the polyimide (PI) coating layer while at the lower substrate *without* PI coating, weak homogeneous anchoring is produced by rubbing along the COP stripes. We model the weak anchoring based on the geometry of the rubbing-induced microgrooves.[10] We emphasize the anchoring condition at the lower substrate is different from that in Ref. 8.

We treat the LC cell as a one-dimensional (1D) system along the z axis. The lower and upper substrates locate at $z=0$ and d, respectively. This 1D treatment considers the effects averaged over the horizontal direction normal to the COP stripes. We consider LC cells in which surface anchoring directions are arranged to stabilize zero-field states of twist angles $\Phi(\mathrm{mod}\,\pi)$, i.e., $\phi(d)-\phi(0)=\Phi(\mathrm{mod}\,\pi)$, where ϕ is the azimuthal angle defined by the director $\mathbf{n}(z)=(\cos\theta\cos\phi,\cos\theta\sin\phi,\sin\theta)$. The d/p ratio is adjusted to make the Φ and $\Phi+\pi$ twist states equally stable. In our coordinate system, the strongly anchored $\mathbf{n}(d)$ at $z=d$ has $\phi(d)=0$, while at $z=0$, $\phi(0)=-\Phi$ and $-\Phi-\pi$, corresponding to $\mathbf{n}(0)=\mathbf{n}_e$ and $-\mathbf{n}_e$ in the Φ and $\Phi+\pi$ twist states, respectively [see Fig. 2(a)]. That means the COP stripes make an angle of $-\Phi(\mathrm{mod}\,\pi)$ with respect to the x axis. In the presence of a strong V_t, the $\mathbf{n}(z)$ configuration is nearly uniform and vertical (for positive dielectric anisotropy) throughout the central part of the cell, but exhibits large elastic distortion (mostly splay bend) near the substrates since surface *polar* anchoring still persists. Applying V_c generates a spatially varying near-surface field that is perpendicular to the COP stripes everywhere. It exerts an azimuthal twisting torque on the surface director $\mathbf{n}(0)$ at the lower substrate $z=0$, hereafter denoted by $\mathbf{n}_s\equiv\mathbf{n}(0)$, whose

a)Electronic mail: phqtz@ust.hk

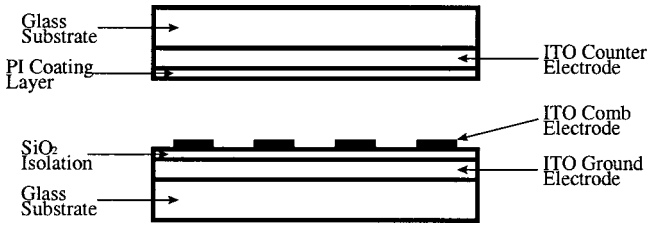

FIG. 1. Schematic diagram of the three-terminal BTN LC cell. COP electrodes are 2 μm wide with a 2μm gap.

azimuthal anchoring can be modeled by a double-well energy potential of the Rapini–Papoular form:[11] $W_\phi[\phi(0)] = \frac{1}{2}A\sin^2[\phi(0)+\Phi]$, where A is the azimuthal anchoring strength. W_ϕ has two local energy minima (easy axes) $\phi(0)=-\Phi$, and $-\Phi-\pi$. A strong near-surface field can break the azimuthal anchoring by orienting $\mathbf{n}_s$ along $\mathbf{n}_d$, the difficult axis that is perpendicular to the easy axes and has the azimuthal angle $\phi_d=-\Phi-\pi/2$ [see Fig. 2(a)], which is the energy maximum separating the two energy wells. This results in a twist angle of $\Phi+\pi/2$.

Dynamic shear flow and field-induced breaking of surface azimuthal anchoring are essential to the existence of the $(\Phi,\Phi+\pi)$ switching bistability in the present BTN display. Switching on V_t and V_c quickly generates an intermediate $\Phi+\pi/2$ twist state with severe splay-bend distortion near the surfaces. Switching off V_t then triggers fast director rotation $\dot{\mathbf{n}}$ near the surfaces. A flow field $\mathbf{v}$ is induced through viscous coupling with $\boldsymbol{\omega}=\nabla\times\mathbf{v}/2$ nearly parallel to $\mathbf{n}\times\dot{\mathbf{n}}$. The whole velocity field can be qualitatively determined from the knowledge of $\boldsymbol{\omega}$ near the surfaces together with the boundary condition $\mathbf{v}=0$ at the surfaces. Throughout the central part of the cell, the nearly uniform $\mathbf{n}(z)$ creates negligible elastic torque. Its rotation is thus dominated by the viscous torque with $\dot{\mathbf{n}}$ along $\boldsymbol{\omega}\times\mathbf{n}$. In this ''backflow'' effect, the directors near the midplane $z=d/2$ rotate in a direction opposed by the elastic coupling across the cell.[3,6] Explicitly, the shear flow produces a transient state with a twist angle $\sim\Phi-3\pi/2$, while the elastic coupling tends to make a twist angle $\sim\Phi+\pi/2$.[12] Now consider the rotation of the director $\mathbf{n}_s$ at the lower substrate $z=0$, where the groove-induced azimuthal anchoring is broken in the intermediate $\Phi+\pi/2$ twist state with $\mathbf{n}_s=\mathbf{n}_d$. Right after V_t and V_c are switched off, $\mathbf{n}_s$ rotates towards $\mathbf{n}_e$ because immediately above $z=0$, $\mathbf{n}(z)$ is close to $\mathbf{n}_d$ but tilts a bit towards $\mathbf{n}_e$. But, soon the elastic coupling in the flow-generated transient $\Phi-3\pi/2$ twist state takes over, the initial rotation towards $\mathbf{n}_e$ is stopped, and then reversed. When the reversed rotation goes across $\mathbf{n}_d$, $\mathbf{n}_s$ escapes from the energy well of $\mathbf{n}_e$ and falls into that of $-\mathbf{n}_e$, with the $\Phi+\pi$ twist state formed at the end. This requires a quick and strong flow in generating the transient $\Phi-3\pi/2$ twist state. Without that, $\mathbf{n}_s$ just remains in the energy well of $\mathbf{n}_e$ and the Φ twist state is formed at the end. These two possibilities are depicted in Fig. 2. Switching bistability can, therefore, be achieved through the control of backflow by adjusting the holding voltage V_t. In addition, the cells must be thin enough to ensure efficient hydrodynamic coupling.[5]

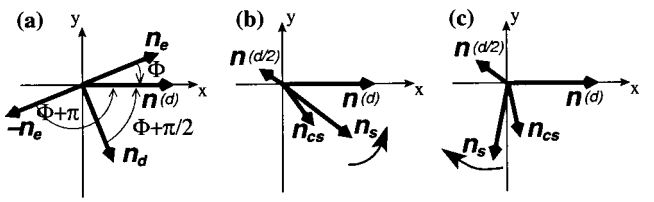

FIG. 2. Director orientation projected onto the *xy* plane. (a) Surface directors $\mathbf{n}(d)$ at $z=d$ and $\mathbf{n}_s=\mathbf{n}_e$, $\mathbf{n}_d$, and $-\mathbf{n}_e$ at $z=0$ in the Φ, $\Phi+\pi/2$, and $\Phi+\pi$ twist states, respectively. (b) $\mathbf{n}_s$ rotating towards $\mathbf{n}_e$ after switching off V_t and V_c. This is coupled to the backflow at $z=d/2$. (c) Elastic effect of the transient twist state stops the rotation of $\mathbf{n}_s$ towards $\mathbf{n}_e$, and causes $\mathbf{n}_s$ to reverse its rotation towards $-\mathbf{n}_e$. Depicted directors are $\mathbf{n}_s\equiv\mathbf{n}(0)$, $\mathbf{n}_{cs}$ close to $z=0$, $\mathbf{n}(d/2)$ at $z=d/2$, and $\mathbf{n}(d)$ anchored at $z=d$.

The $(\Phi,\Phi+\pi)$ switching bistability was observed in cells of $d=2.5\,\mu$m and $\Phi=-22.5°$.[13] The existence of switching bistability allows a wide range for the value of Φ. Here, Φ was selected to optimize the optical properties.[13] The driving wave form consists of two pulses $V_t(t)$ and $V_c(t)$. They first jump from zero to two holding voltages V_t and V_c, respectively, and then last for the same time duration before being suddenly switched off. We scanned V_t and V_c to obtain the parameter space working for the $(\Phi,\Phi+\pi)$ switching. We focused on the regime of complete breaking of surface azimuthal anchoring by putting V_c above a threshold ~40 V. The switching to the $\Phi+\pi$ twist state was observed using a high holding voltage V_t^H, while the switching to the Φ twist state was observed using a low holding voltage V_t^L. It was verified that $V_t^L<V_t^S$ and $V_t^H>V_t^S$ where $V_t^S\simeq 10$ V can be regarded as a critical voltage for the switching bistability. This agrees with our physical picture that the relaxation from the $\Phi+\pi/2$ to the $\Phi+\pi$ state needs a strong flow that can be induced by turning off a large holding voltage V_t. However, as V_t goes too high, the surface polar anchoring becomes partially broken. The backflow effect is then weakened as a result of the reduced splay-bend distortion near the surfaces. This is consistent with the observation that the switching to the $\Phi+\pi$ state becomes unstable for $V_t\sim 2V_t^S$. In fact, the switching to the Φ state was observed when $V_t>2V_t^S$, even if a very low V_c was applied. This falls into the regime of hydrodynamically coupled asymmetric breaking of surface polar anchorings studied in Ref. 5.

We model the switching bistability in the regime of azimuthal anchoring breaking. In numerical computation,[3] the values of the three elastic constants and the six viscosity coefficients are taken from Refs. 3 and 6, suitable for MBBA, since very few data are available for the complete set of those parameters. Using other values (suitable for PAA or 5CB) leads to a slight quantitative change in the numerical results. The dielectric constants are set to be $\epsilon_\parallel=15$ and $\epsilon_\perp=5$, corresponding to the large dielectric anisotropy ($\epsilon_a\simeq 10$) of the LC materials used in the experiments. We first obtain the intermediate $\Phi+\pi/2$ twist state by minimizing the free energy $\int_0^d dz[f_{\rm el}-E_z(z)/D_z/8\pi]+W_\theta[\theta(0)]$, where $f_{\rm el}$ is the curvature elastic energy density, $-E_z(z)D_z/8\pi$ is the field-induced free-energy density, and W_θ, a function of $\theta(0)$, is a polar anchoring potential at $z=0$. Here, E_z is the z component of the electric field satisfying $V_t=\int_0^d E_z(z)dz$, and $D_z=\epsilon_{zz}E_z$ is the z component of the electric displace-

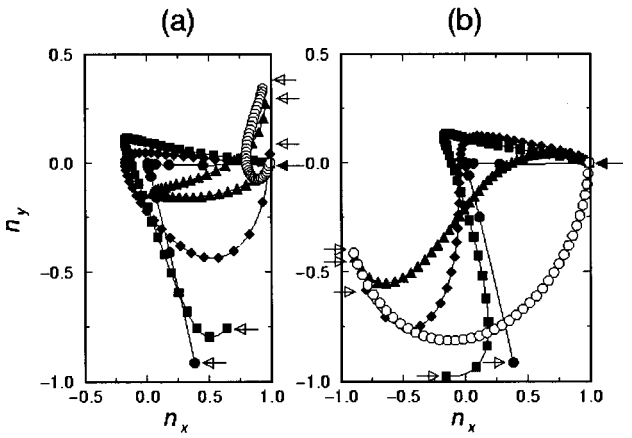

FIG. 3. Relaxation starting from the $\Phi+\pi/2$ state. (a) Towards the Φ state for $V_t^L=8$ V. (b) Towards the $\Phi+\pi$ state for $V_t^H=12$ V. Configurations at time $t=0$ ($\Phi+\pi/2$ state, solid circle), 0.005 (square), 0.01 (diamond), 0.02 (triangle), and 0.1 (empty circle) are depicted (time in unit of $\alpha_4 d^2/K_{\text{splay}}$). Marks are put at 41 equally spaced levels, first at $z=0$ (hollow arrow) and last at $z=d$ (filled arrow).

ment field, which is z independent. A large anchoring strength is used in W_θ to keep $\theta(0)$ small ($\sim 10°$) and maintain the surface polar anchoring at $z=0$. To reflect the complete breaking of azimuthal anchoring, $\phi(0)$ is set to be $-\Phi-\pi/2$. This simple treatment relies on $\phi(0)=\phi_d$ to take into account of the effect of the V_c-generated field, which is close to $z=0$ and orients $\mathbf{n}_s$ along $\mathbf{n}_d$. At the rubbed PI-coated upper substrate, a strong anchoring condition is applied to $\mathbf{n}(d)$ by using the fixed values $\theta(d)=8°$ and $\phi(d)=0°$.

We then turn to the relaxation starting from the $\Phi+\pi/2$ state after V_t and V_c are switched off. We solve the Ericksen–Leslie equations[14] under the boundary conditions that at $z=d$, $\mathbf{n}(d)$ is fixed while at $z=0$, $\mathbf{n}_s$ is governed by a phenomenological dynamic equation,[15] $\gamma_s \mathbf{n}_s \times \dot{\mathbf{n}}_s = \boldsymbol{\tau}_e + \boldsymbol{\tau}_s$, where γ_s is the surface viscosity coefficient, $\boldsymbol{\tau}_e$ the torque from f_{el}, and $\boldsymbol{\tau}_s$ the torque from both W_ϕ and W_θ. Here, W_ϕ is important in determining the motion of $\phi(0)$, and thus the direction of relaxation, while W_θ simply constrains $\theta(0)$ around its equilibrium. We find that the final state of relaxation is selected by the holding voltage V_t under which the intermediate $\Phi+\pi/2$ twist state is stabilized. That means, given an anchoring strength A, there exists a critical voltage V_t^S, for $V_t<V_t^S$ the final state is the Φ twist state while for $V_t>V_t^S$ the final state is the $\Phi+\pi$ twist state, as illustrated in Fig. 3. It is readily seen that where the relaxation ends up is decided in its early stage. Given $A\simeq 0.03\,\text{erg/cm}^2$, we obtain $V_t^S\simeq 10$ V. Similarly, given the holding voltage V_t, there exists a critical anchoring strength A^S, for $A>A^S$ the final state is the Φ twist state while for $A<A^S$ the final state is the $\Phi+\pi$ twist state. These numerical results agree with both the theoretical picture and the experimental observation. Finally, it is interesting to look at $A\simeq 0.03\,\text{erg/cm}^2$, the anchoring strength corresponding to the experimental value of the critical field, $V_t^S\simeq 10$ V. According to Ref. 10, the extrapolation length for this azimuthal anchoring strength is determined by the pitch and depth of the rubbing-induced grooves. For elastic constants $K\sim 3\times 10^{-7}$ dyn, the extrapolation length is $K/A\simeq 0.1\,\mu$m, which leads to the relation $\lambda^3/u^2\simeq 4\pi^3\times 0.1\,\mu$m, where λ is the period of groove alignment and u the groove depth. Assuming $u\simeq 0.1\lambda$ then gives $\lambda\sim 0.1\,\mu$m and $u\sim 0.01\,\mu$m, both in the physically acceptable range.

In summary, we have presented a theoretical picture for the $(\Phi,\Phi+\pi)$ switching bistability in three-terminal BTN displays. The dynamic flow and broken surface anchoring are essential to the realization of the switching bistability experimentally observed. The agreement between experimental observation and theoretical calculation is fairly satisfactory.

This work was supported by the Hong Kong Innovation and Technology Fund. One of the authors (T.Q.) was also supported by Project No. HKUST6133/97P.

[1] D. W. Berreman and W. R. Heffner, J. Appl. Phys. **52**, 3032 (1981).
[2] T. Tanaka, Y. Sato, A. Inoue, Y. Momose, H. Nomura, and S. Iino, Asia Display **95**, 259 (1995).
[3] T. Z. Qian, Z. L. Xie, H. S. Kwok, and P. Sheng, Appl. Phys. Lett. **71**, 596 (1997).
[4] Z. L. Xie, Y. M. Dong, S. Y. Xu, H. J. Guo, and H. S. Kwok, J. Appl. Phys. **87**, 2673 (2000).
[5] I. Dozov, M. Nobili, and G. Durand, Appl. Phys. Lett. **70**, 1179 (1997).
[6] C. Z. van Doorn, J. Appl. Phys. **46**, 3738 (1975); D. W. Berreman, *ibid.* **46**, 3746 (1975).
[7] G. P. Bryan-Brown, C. V. Brown, I. C. Sage, and V. C. Hui, Nature (London) **392**, 365 (1998).
[8] J. X. Guo, Z. G. Meng, M. Wong, and H. S. Kwok, Appl. Phys. Lett. **77**, 3716 (2000).
[9] Z. G. Meng, H. S. Kwok, and M. Wong, Proceedings of International Display Works, Sendai, Japan, 1999, p. 125 (unpublished).
[10] D. W. Berreman, Phys. Rev. Lett. **28**, 1683 (1972).
[11] A. Rapini and M. Papoular, J. Phys. Colloq. **30**, C4 (1969).
[12] The $(\pi, -3\pi/2)$ switching bistability has already been verified for the cells of strong anchoring conditions; see Ref. 3.
[13] Φ was selected for optical optimization; see H. S. Kwok, J. Appl. Phys. **80**, 3687 (1996).
[14] J. L. Ericksen, Phys. Fluids **9**, 1205 (1966); F. M. Leslie, Q. J. Mech. Appl. Math **19**, 357 (1966).
[15] See G. E. Durand and E. G. Virga, Phys. Rev. E **59**, 4137 (1999); here, the value of γ_s is unknown and $\gamma_s=\alpha_4 l_s$ is used with $\alpha_4\sim 0.1$ P being the fourth Leslie coefficient and $l_s\simeq 100$ Å a molecular length scale.